



City Research Online

City, University of London Institutional Repository

Citation: Elks, P. M., van Eeden, F. J., Dixon, G., Wang, X., Reyes-Aldasoro, C. C., Ingham, P., Whyte, M., Walmsley, S. R. & Renshaw, S. A. (2011). Activation of hypoxia-inducible factor-1 α (Hif-1 α) delays inflammation resolution by reducing neutrophil apoptosis and reverse migration in a zebrafish inflammation model. *Blood*, 118(3), pp. 712-722. doi: 10.1182/blood-2010-12-324186

This is the accepted version of the paper.

This version of the publication may differ from the final published version.

Permanent repository link: <https://openaccess.city.ac.uk/id/eprint/5507/>

Link to published version: <https://doi.org/10.1182/blood-2010-12-324186>

Copyright: City Research Online aims to make research outputs of City, University of London available to a wider audience. Copyright and Moral Rights remain with the author(s) and/or copyright holders. URLs from City Research Online may be freely distributed and linked to.

Reuse: Copies of full items can be used for personal research or study, educational, or not-for-profit purposes without prior permission or charge. Provided that the authors, title and full bibliographic details are credited, a hyperlink and/or URL is given for the original metadata page and the content is not changed in any way.

City Research Online:

<http://openaccess.city.ac.uk/>

publications@city.ac.uk

Abstract

The oxygen sensing transcription factor HIF-1 α plays a critical role in the regulation of myeloid cell function. The mechanisms of regulation are not well understood, nor the phenotypic consequences of HIF modulation in the context of neutrophilic inflammation. Species conservation across higher metazoans enables the use of the genetically tractable and transparent zebrafish embryo to study *in vivo* resolution of the inflammatory response. Using both a pharmacological approach known to lead to stabilization of HIF-1 α , and selective genetic manipulation of zebrafish HIF-1 α homologues we sought to determine the roles of HIF-1 α in inflammation resolution. Both approaches reveal that activated Hif-1 α delays resolution of inflammation following tail transection in zebrafish larvae. This delay can be replicated by neutrophil specific Hif activation, and is a consequence of both reduced neutrophil apoptosis, and increased retention of neutrophils at the site of tissue injury. Hif-activated neutrophils continue to patrol the injury site during the resolution phase, when neutrophils would normally migrate away. Site-directed mutagenesis of Hif *in vivo* reveals that hydroxylation of Hif-1 α by Phd hydroxylases critically regulates the Hif pathway in zebrafish neutrophils. Our data demonstrate that Hif-1 α regulates neutrophil function in complex ways during inflammation resolution *in vivo*.

Introduction

Neutrophilic inflammation is of fundamental importance in the innate immune response to bacterial and fungal infection in vertebrates, and can be initiated by sterile tissue injury. Irrespective of its aetiology, inflammation must resolve in a timely fashion to avoid damage to surrounding tissues.¹ Persisting, non-infectious inflammation is the hallmark of inflammatory diseases, a major cause of morbidity and mortality in the developed world. The resolution phase of inflammation is critical to the restoration of normal tissue function following an inflammatory response, and thus has a central role in determining the outcome of inflammation.² Despite the central place of failed resolution in the pathogenesis of inflammatory disease, much remains to be known about the cellular and molecular events involved.

While neutrophil apoptosis, and subsequent uptake and removal by macrophages (efferocytosis), is well documented as a disposal route for inflammatory neutrophils,³⁻⁵ there is emerging evidence that other mechanisms may also contribute to certain types of inflammation resolution. In the lung, some neutrophils are lost into the airways and expectorated⁶ and in rheumatoid arthritis, neutrophils may leave the inflammatory site while still alive and re-enter the circulation.⁷ Neutrophils can also be removed by migration through tissues away from the infection site; a process termed retrograde chemotaxis, or reverse migration.⁸⁻¹⁰ This process is most widely characterized in the zebrafish embryo and is less well studied in mammalian systems.

Each of these aspects of inflammation resolution may contribute to the removal of neutrophils, and be influenced by a range of extracellular signals encountered by neutrophils at the site of inflammation, including cytokines,^{11,12} bacterial products,^{12,13} and low oxygen tensions.¹⁴⁻¹⁶ Physiological hypoxia is important since it induces both extended survival and preserved activity in neutrophils. Hypoxia exerts its effects in part through stabilization of Hypoxia Inducible Factor (HIF), with activation of the HIF pathway in murine myeloid cells by myeloid specific *Vhl* knockout leading to increased myeloid cell recruitment.¹⁷ HIF signaling can be activated in normoxia by exposure of myeloid cells to bacterial products, demonstrating the fundamental importance of this pathway to immune cell function.¹⁸ The effects of HIF-1 α activation and silencing on resolution of neutrophilic inflammation have yet to be fully characterized, especially in an *in vivo* setting.

Three HIF- α isoforms have been identified in humans, of which HIF-1 α is a key regulator of neutrophil function and lifespan.¹⁷⁻¹⁹ HIF-1 α stability is regulated by a group of oxygen sensitive enzymes: prolyl hydroxylases (PHDs) and factor inhibiting HIF (FIH). Oxygen dependent PHD activity

leads to degradation of HIF-1 α via a ubiquitin ligase complex co-ordinated by the von Hippel Lindau (VHL) protein.²⁰⁻²² In contrast, hypoxia reduces PHD activity, stabilising HIF-1 α , which joins a nuclear complex with the constitutively expressed HIF- β (or aryl hydrocarbon nuclear translocator, ARNT) and transduces the cellular response.²²⁻²⁴ The HIF pathway can be manipulated pharmacologically using non-specific inhibitors of PHD enzymes, for example dimethyloxaloylglycine (DMOG), leading to stabilization of HIF-1 α *in vitro*.²⁵ Such pan-hydroxylase inhibitors lack specificity, however, with potential widespread effects on cellular physiology.

Here, using a transgenic zebrafish line expressing a neutrophil specific reporter gene,²⁶ we investigate the effects of pharmaceutical and genetic manipulation of Hif-1 α activity on neutrophil behaviour *in vivo*. We show for the first time that the resolution of neutrophilic inflammation *in vivo* is delayed following DMOG treatment in a whole organism model. We show this delay in resolution is a consequence both of a decrease in neutrophil apoptosis, and of increased retention of neutrophils at the site of inflammation. Furthermore, using dominant active and dominant negative variants of the two zebrafish homologues of HIF-1 α (Hif-1 α a and Hif-1 α b) we show timely resolution of neutrophilic inflammation is dependent on prolyl hydroxylation of Hif-1 α b, demonstrating the importance of the HIF pathway in determining the outcome of inflammation *in vivo*.

Methods

Fish husbandry

Two neutrophil specific fluorescent zebrafish lines were used: *Tg(mpx:GFP)i114*²⁶ and *Tg(lyz:GAL4.VP16)i252;Tg(UAS-Elb:Kaede)s1999t* subsequently termed *mpx:GFP* and *lyz:Kaede*. Zebrafish strains were maintained according to standard protocols.²⁷ Adult fish were maintained on a 14/10 hour light/dark cycle at 28°C in UK Home Office approved facilities in the MRC CDBG aquaria at the University of Sheffield.

Inflammation assay

Inflammatory responses were elicited in zebrafish embryos by tail transection as previously described.²⁶ Embryos were anesthetized at two or three days post-fertilization (dpf) by immersion in 0.168 mg/ml Tricaine (Sigma-Aldrich, St. Louis, MO) and transection of the tail was performed with a scalpel blade briefly immersed in the chemoattractant f-met-leu-phe (100nM, Sigma-Aldrich). Treatment with 100 μ M DMOG (or DMSO vehicle control) was performed by immersion at 4 hours post injury (hpi), or for recruitment assays for 2 hours before injury. Neutrophils were counted at the site of transection at 6, 24 and 48 hpi using a fluorescent dissecting stereomicroscope (Leica Microsystems GmbH, Wetzlar, Germany) as described previously.²⁶ Where possible, counting was performed blind to experimental conditions.

Apoptosis assays

Rates of apoptosis were assessed blindly by TUNEL/TSA or by anti-active caspase-3/TSA staining, as previously described.^{28,29}

Mpx:GFP embryos were injured at 3dpf (2dpf in the case of RNA injected embryos) and 10dpf. Embryos were treated with DMSO/DMOG at 4hpi, and fixed at 12hpi in 4% paraformaldehyde. TUNEL (ApopTag Red, Chemicon, Millipore, Billerica, MA) staining labeled apoptotic cells with red fluorescence and TSA (TSAplus kit, Fluorescence Systems, Perkin Elmer Inc., Waltham, MA) staining labeled neutrophils with fluorescein green fluorescence. Anti-active caspase-3 (R&D Systems, Minneapolis, MN) staining with a fluorescein secondary antibody (Alexa Fluor 488, goat anti-rabbit IgG, Invitrogen, Carlsbad, CA) gave green fluorescence. Neutrophils were labeled with red fluorescence using Cyanine-3 TSA (TSAplus kit, Fluorescence Systems, Perkin Elmer Inc.).

Neutrophils in the tail transection region were imaged on an UltraVIEWVoX spinning-disk confocal microscope (Perkin Elmer Inc.) and apoptosis assessed by the percentage of TSA positive neutrophils labeled with TUNEL or active caspase-3.

Development of a stable *Tg(lyz:GAL4.VP16)i252* transgenic line

The Tol2kit multisite Gateway-based transposon system was used to make a transgenic construct from which a stable line was raised.³⁰ 11 kilobases of the *lysosyme C* promoter (kindly provided by Phil Crosier),¹⁰ was cloned into the p5E-MCS entry vector (Xho-I and Sma-I sites). An LR Clonase II Plus Enzyme (Invitrogen) Gateway reaction was performed with the resulting p5E-*lyz* along with, pME-Gal4VP16, p3E-polyA inserted into pDestTol2pA2 to produce *lyz:Gal4VP16* construct. This construct was co-injected with tol2-transposase RNA into zebrafish one-cell stage embryos to create the *Tg(lyz:GAL4.VP16)i252* transgenic line.

Photoconversion of neutrophil specific Kaede protein

Tail transection of *lyz:Kaede* larvae was performed at 2 or 3dpf as previously described.²⁶ Embryos were raised to 6hpi and mounted in 1% low-melting point agarose (Sigma-Aldrich). A Perkin Elmer UltraVIEW PhotoKinesis™ device on an UltraVIEWVoX spinning disk confocal microscope (Perkin Elmer Inc.) was used to photoconvert the Kaede labeled cells using 120 pulses of the 405nm laser at 40% laser power (optimised in previous experiments, data not shown). Embryos were transferred to a Nikon Eclipse TE2000-U Inverted Compound Fluorescence Microscope (Nikon, Tokyo, Japan) where a Hamamatsu 1394 ORCA-ERA camera (Hamamatsu Photonics Inc. Hamamatsu City, Japan) was used to capture a timelapse series. Cells fluorescing in the red channel were then tracked over a 3.5 hour period.

Neutrophil tracking

Tracking analysis was performed in Volocity 5 (Improvision, Perkin Elmer Inc.), using the intensity of fluorescence to identify individual labeled neutrophils over time.

Morpholino knockdown of *arnt-1*

The *arnt-1* morpholino (Genetools, Philomath, OR) was used as previously reported.³¹ A standard control morpholino (Genetools) was used as a negative control.

***hif-1α* cloning**

Zebrafish 2dpf RNA purified using TRIzol (Invitrogen, Carlsbad, CA) was used for RT-PCR cloning of zebrafish *hif-1aa* and *hif-1ab* (using primers in Table S1) using Pfuusion polymerase (Finnzymes, Espoo, Finland). These were cloned into TOPOBlunt (Invitrogen) and were subsequently subcloned into pCS2+ (Invitrogen) for RNA synthesis and *in situ* hybridization expression studies.

Dominant negative forms of *hif-1aa* and *hif-1ab* were generated using primers amplifying DNA corresponding to amino acids 1-330 of human HIF-1α.³² Dominant active forms of *hif-1aa* and *hif-1ab* were generated by successive rounds of site-directed mutagenesis.³³⁻³⁵ In each round one of the hydroxylation sites were mutated into non-hydroxylatable amino acids as previously described in human HIF-1α.³³⁻³⁵

Dominant negative and dominant active RNAs were transcribed (mMessageMachine, Ambion, Life Technologies Corp., Carlsbad, CA) and micro-injected into zebrafish embryos at the one cell stage as previously described.^{27,36} A *phd-3 in situ* hybridization was performed to assess the function of dominant *hif-1α* variants, using previously described methods.^{36,37}

Development of a stable *Tg(UAS:da-hif-1αb-IRES-GFP)i218* transgenic line

Dominant active *hif-1αb* was cloned into the middle entry pME-MCS. An LR Clonase (Invitrogen) Gateway reaction was performed with p5E-UAS, pME-*da-hif-1αb* and p3E-IRES-EGFPpA inserted into pDestTol2pA2. The resulting plasmid was microinjected with tol2-transposase RNA into one-cell stage embryos. IRES-GFP expression was weak, so founders were screened by heart marker GFP

expression. The resulting *Tg(UAS:da-hif-1 α b-IRES-GFP)i218* is subsequently referred to as *UAS:da-hif-1 α b*.

Functional Hif expression was tested in *UAS:da-hif-1 α b*, by injection with a *cmv:Gal4VP16-IRES-nlsEGFP* construct, made from the *tol2kit* as previously described.³⁰ Injected larvae were screened for expression of nlsEGFP at 3dpf and a *phd-3 in situ* hybridization was performed to assess levels of Hif-1 α signaling. To investigate the effects of *da-hif-1 α b* expression on the resolution of neutrophilic inflammation *UAS:da-hif-1 α b* were crossed to *Tg(lyz:Gal4)i252* fish to generate double transgenic embryos identified by the presence of GFP heart marker and mCherry labeled leukocytes.

Statistical analysis

Data were analyzed (Prism 5.0, GraphPad Software, San Diego, CA) using unpaired, two-tailed t-tests for comparisons between two groups and one-way ANOVA (with Bonferonni post-test adjustment) for other data.

Results

DMOG treatment delays resolution of inflammation

Following tail transection in *mpx:GFP* embryos at 3dpf, neutrophil numbers can be assessed by counting fluorescent cells, visible in association with the site of injury. Neutrophils numbers act as a measure of the magnitude of the inflammatory response as they are its main cellular component. Neutrophils are recruited early, with numbers peaking around 6 hours,²⁶ followed by spontaneous resolution of this neutrophilic inflammation over 24 hours (Figure 1A). Macrophages are recruited later and persist longer.³⁸

Because of the known effects of the pan-hydroxylase inhibitor DMOG on neutrophil apoptosis, we hypothesized that DMOG would delay inflammation resolution in the zebrafish tailfin model. Agents delaying neutrophil apoptosis have been shown to delay inflammation resolution in this model when added once neutrophils have been recruited.²⁸ We therefore added 100 μ M DMOG at 4hpi, and observed the effects on inflammation resolution. Treatment with DMOG caused a significant increase in neutrophil numbers at 24hpi (Figure 1B, 1C-D) compared to DMSO treated controls (Figure 1A, 1C-D) from the same clutch of embryos, but numbers had decreased to basal levels by 48hpi, despite persistence of Hif signaling at 48hpi, as assessed by *in situ* hybridization expression of the target gene *phd-3* (Figure S1A). There were no additional effects of DMOG on neutrophil distribution throughout the embryo (Figure 1E), nor any increase in total neutrophil number (Figure S1B). DMOG dose and timing of administration were assessed and found to be optimal (Figure S1C-D).

Recruitment of neutrophils was assessed at 6hpi and was unchanged by DMOG treatment (Figure 1F), confirming that the differences seen in percentage change in neutrophil number from 6 to 24 hours (a measure of inflammation resolution) in DMOG treated embryos, is independent of effects on neutrophil recruitment (Figure 1G).

Neutrophil counts do not take account of changes in the migration behaviour of neutrophils, which may be affected by hydroxylase inhibition. We therefore assessed the speed and meandering of neutrophil migration towards the site of tail transection by *in vivo* tracking of *mpx:GFP* neutrophils over 1 hour during the recruitment phase using 3D videotimelapse microscopy (Figure 1H). This tracking technique was sensitive enough to detect changes in neutrophil recruitment after treatment with the chemoattractant fMLP (Figure S2A-B). After DMOG treatment, however, no significant difference in neutrophil speed (Figure 1I) or meandering index (Figure 1J) was observed when compared to vehicle only controls during the recruitment phase.

DMOG treatment decreases neutrophil apoptosis and retains neutrophils at the inflammatory site

DMOG treatment increased the number of neutrophils at the site of tail transection at 24hpi, but the mechanisms behind this delay in resolution remained unknown. Neutrophils were never seen to leave

the zebrafish body through the wound margin or elsewhere, and it is reasonable to conclude that loss of neutrophils from the larva is not important in this model. We therefore assessed the effects of DMOG both on levels of neutrophil apoptosis at the transection site, and on migration of neutrophils away from it.

Neutrophil apoptosis was quantified using TUNEL staining to identify apoptotic cells, in combination with a fluorescent histochemical stain to identify neutrophils, as previously reported.^{28,29,39} Post-mortem TSA staining was used in preference to GFP imaging, since we have previously shown GFP fluorescence is lost during neutrophil apoptosis.²⁸ In DMOG treated larvae there was a significant decrease in apoptotic neutrophils at the transection site when compared to that of DMSO treated larvae at 3dpf (Figure 1K). The rates of apoptosis seen are comparable to those in other studies of zebrafish neutrophil apoptosis,²⁸ and to published rates of detectable apoptosis in other models.⁴⁰ Because levels of detectable neutrophil apoptosis are low, these events are scarce in fixed embryos at a single timepoint, presumably reflecting the short lifespan of an apoptotic neutrophil *in vivo*. Therefore this experimental result was confirmed at 10dpf where numbers of neutrophils are higher using both TUNEL and anti-active caspase-3 staining (Figure S3A-B).

In order to investigate the migration of neutrophils away from the transection site, *lyz:Kaede* transgenic fish were used. *lyz:Kaede* fish use the lysozyme C promoter to drive GAL4, which drives expression of Kaede, a photoconvertible protein that fluoresces in the red channel following exposure to 405nm excitation.⁴¹ This allows individual cells, or cells within a certain area, to be converted from green to red fluorescence and tracked over time. Tailfin transection was performed in *lyz:Kaede* transgenic zebrafish at 3dpf, and at 6hpi the neutrophils present at the transection site were photoconverted to red fluorescence and tracked over the next 3.5 hours (Figure 2A). Embryos treated with DMOG had significantly fewer red neutrophils moving away from the injury site than DMSO controls (Figure 2B-D). Not only were more neutrophils in DMSO treated embryos moving away from the injury site, but they were moving further away than those treated with DMOG (Figure S4A).

To further investigate neutrophil movement at the injury site after DMOG treatment, a small area of between 5-10 neutrophils located at the dorsal side of the midline near the wound was photoconverted at 6hpi (Figure 3A). It was observed that DMSO treated neutrophils tended to migrate away from the injury site whilst DMOG treated neutrophils favoured migration along the injury edge (Figure 3B). This was independent of measurements of speed and meandering, which remained unchanged after treatment (Figure 3C). Over 3.5 hours of tracking, neutrophils migrated out of the photoconverted region at the same rate in both DMSO and DMOG treated individuals (Figure 3D). Fewer neutrophils migrate away from the injury site in DMOG treated individuals than in DMSO controls (Figure 3E), whilst more neutrophils in DMOG treated embryos moved down the injury site ventral of the photoconverted region (Figure 3F). This is consistent with DMOG treated neutrophils patrolling the injury site, rather than moving away.

DMOG-induced delay in resolution is blocked by *arnt-1* morpholino and by dominant negative *hif-1ab*

Given the potential for non-specific effects of competitive hydroxylase inhibition by DMOG and the lack of selective inhibitors of individual PHD enzymes, we sought to investigate the HIF-1 α dependence of hydroxylase inhibition. ARNT-1 (or HIF-1 β) is a crucial binding partner of HIF-1 α , and *arnt-1* morpholino³¹ will block Hif signaling. In the morpholino experiments, tail transection was performed at 2dpf, to increase the likelihood that the morpholino would remain active during the experiment. The 2dpf tail transection model retains the same features as the 3dpf model used in other studies,^{26,28,42} and was used for all morpholino and RNA injection experiments below. In control morpholino injected larvae, DMOG increased neutrophil numbers at 24hpi. Treatment with DMOG after *arnt-1* morpholino injection, however, caused no significant increase in neutrophil numbers at 24hpi (Figure 4A), supporting the Hif dependence of the DMOG effect.

A truncated form of human HIF-1 α has been previously shown to block HIF-1 α signaling in cell culture.³² We generated analogous constructs for the zebrafish homologues, *hif-1aa* and *hif-1ab*. These

were expressed in all cells of the embryo by RNA injection at the one cell stage. We showed dominant negative *hif-1a* was able to block activation of the HIF pathway by DMOG as late as 56hpf, indicated by a decrease in *phd-3* expression (Figure S5).⁴³ Dominant negative *hif-1a* abrogated the DMOG induced increase in neutrophil numbers at the transection site at 24hpi (Figure 4B), with no effect on wholebody neutrophil numbers (Figure 4C). Dominant negative *hif-1ab* alone was sufficient to block the DMOG delay in resolution of neutrophilic inflammation (Figure 4B), with *hif-1aa* having no effect on inflammation (Figure 4B). TUNEL staining showed that there was no significant difference in levels of neutrophil apoptosis in embryos injected with dominant negative *hif-1a* (Figure 4D).

In order to investigate the effect on neutrophil retention at the inflammatory site, *lyz:Kaede* embryos were injected with dominant negative *hif-1ab* RNA and neutrophils at the inflammatory site were photoconverted. Neutrophil movement away from the wound was investigated at 6hpi after tail transection at 2dpf. In phenol red injected negative control embryos, DMOG treatment caused fewer neutrophils to leave the site of transection (Figure S4B), as was observed at 3dpf. However, in embryos injected with dominant negative *hif-1ab*, DMOG treated embryos had similar numbers of neutrophils migrating away from the site of transection as the DMSO treated individuals (Figure 4E-F). The neutrophils that did move away, moved similar distances away from the injury site in treatment groups (Figure S4C). Therefore dominant negative *hif-1a* is able to negate the DMOG-induced delay in resolution partially by restoring the normal pattern of neutrophil movement away from the wound edge.

Dominant active *hif-1ab* delays resolution of neutrophilic inflammation

Dominant active forms of Hif-1 α and Hif-1 β were generated by mutation of conserved proline hydroxylation sites for Phd and the asparagine hydroxylation site for Fih (Figure 5A). In mammalian studies, these mutations render HIF-1 α resistant to hydroxylation by oxygen sensitive hydroxylases, leading to stabilization of HIF-1 α .³³⁻³⁵ In zebrafish larvae expressing dominant active *hif-1a* by RNA injection, Hif signaling was upregulated, shown by increased *phd-3* expression (Figure S5). In addition, an increase in neutrophil number at 24hpi was observed in dominant active *hif-1a*, DMSO treated embryos, with neutrophil numbers comparable to DMOG treated, mock-injected siblings (Figure 5B). As with dominant negative *hif-1a*, dominant active *hif-1ab* alone recapitulated the effects of DMOG on 24hpi neutrophil numbers present at the transection site (Figure 5B). Neither dominant active nor negative *hif-1aa* had any effect in these assays. *In situ* hybridization expression of wildtype *hif-1aa* and *hif-1ab* showed similar expression patterns, although in general *hif-1aa* appeared to be expressed at a lower level than *hif-1ab* (Figure S6).

Dominant active *hif-1a* injection was associated with increased wholebody neutrophil numbers at 2dpf (Figure 5C) suggesting activation of Hif signaling might regulate total neutrophil numbers *in vivo*. Since HIF is activated by infection, this effect might contribute to the increase in neutrophils seen during infections however, this increase in wholebody neutrophil number did not cause an increase in neutrophil recruitment to the injury site at 6hpi (Figure 5D). Like DMOG, dominant negative and dominant active forms of *hif-1a* caused no significant changes in neutrophil speed or meandering index during the recruitment phase (Figure S2C-D).

TUNEL staining showed that there was a significant decrease in levels of neutrophil apoptosis in embryos injected with dominant active *hif-1a* (Figure 5E), similar to that observed in DMOG (Figure 1K). Neutrophil migration away from the injury site was assessed as with *lyz:Kaede*. Fewer neutrophils move out of the injury site in dominant active *hif-1a* injected embryos compared to phenol red injected controls (Figure 5F).

Each hydroxylation site of Hif-1 β was mutated individually and RNA injected into *mpx:GFP* larvae to assess their effects on neutrophil retention at 24hpi. Mutation of either of the two Phd target proline residues was sufficient to significantly increase the neutrophil numbers at the site of transection at 24hpi to the same or greater level as DMOG treatment (Figure 5G). Mutation of the Fih target asparagine had no effect on neutrophil numbers at 24hpi (Figure 5G).

To confirm the effects of Hif activation act within the neutrophil itself, a stable transgenic line expressing dominant active *hif-1ab* under the UAS promoter was generated (*UAS:da-hif-1ab*). This line

was shown to express active Hif when driven by an injected *cmv:GAL4* construct, demonstrated by increased *phd-3* expression (Figure S7). Dominant active *hif-1ab* was expressed in neutrophils by crossing *UAS:da-hif-1ab* with the *lyz:Gal4* line described above. Following tail transection at 3dpf, neutrophils were counted at 24hpi after fluorescent TSA. Neutrophil numbers at 24hpi are elevated in embryos with the heart marker (i.e. *da-hif-1a* positive) compared to heart marker negative siblings (Figure 5H). As with dominant active *hif-1a* RNA experiments, levels of apoptosis are significantly reduced in *da-hif-1a* positive transgenics compared to controls (Figure 5I).

Discussion

In these studies we investigated the role of the HIF pathway in modulating neutrophilic inflammation *in vivo*. Although a number of *in vitro* studies have shown effects on neutrophil function and lifespan,^{14-16,19} there has been no previous study of the effects of HIF signaling on neutrophil behaviour during inflammation *in vivo*. We found recruitment of neutrophils to the injury site was unaffected by hydroxylase inhibition, and in addition, the pattern of neutrophil localization was unaltered in uninjured embryos. Neutrophil migration properties including speed and meandering of neutrophils during the recruitment phase were also not affected. DMOG did, however, cause a delay in the resolution of inflammation in association with an increase in HIF signaling. HIF signaling pathways therefore modulate the resolution rather than recruitment phase of inflammation. The number of neutrophils at the transection site in DMOG treated embryos had reached basal levels by 48hpi, suggesting that the abrogation of hydroxylase activity delays rather than prevents the resolution of inflammation.

There are two plausible explanations for the decrease in inflammation resolution observed in DMOG treated zebrafish embryos: neutrophils are actively retained at the site of injury and/or neutrophil apoptosis is suppressed. Movement of neutrophils away from sites of injury and infection, by reverse migration, has been reported in a number of zebrafish studies.⁸⁻¹⁰ A similar phenomenon has been reported in some mammalian systems, although the underlying mechanisms are less well understood.⁷ Cell tracking experiments were performed to assess movement of neutrophils away from the wound region. In DMOG treated embryos, fewer labeled neutrophils left the site of transection over a 3.5 hour period during the resolution phase of inflammation and neutrophils travelled a shorter distance away from the wound zone. These effects of DMOG were blocked by dominant negative and replicated by dominant active Hif constructs, indicating Hif signaling retained neutrophils in the wound zone during the resolution phase. By labeling a small population of cells at the injury site we were able to show that the same number of neutrophils remain in the labeled region in DMOG treated embryos in the resolution phase, and that neutrophils migrate with the same speed and meandering index. The difference between these populations is purely a difference in the direction of the migrating neutrophils. Blocking hydroxylases led to more neutrophils patrolling the injury site rather than moving away from the injury site. This change in migration direction may reflect a differential response of neutrophils to existing chemotactic gradients, perhaps as a result of altered chemokine receptor expression.⁴⁴ It is unlikely that global activation of Hif signaling causes a change in the chemical gradients at the injury site, as neutrophil specific expression of dominant Hif-1a led to persisting inflammation. The decrease in reverse migration after Hif activation is likely to be partly responsible for the decrease in the resolution of neutrophilic inflammation. To our knowledge, this is the first report of the modulation of a genetic pathway directly altering the migratory behaviour of neutrophils specifically during inflammation resolution. Whether this represents a global effect of HIF signaling on inflammation resolution, or whether it is specific to zebrafish will require careful experimentation in emerging models of *in vivo* inflammation in mammalian systems.

In addition, DMOG treatment caused a modest but significant decrease in the levels of neutrophil apoptosis in the resolution phase of inflammation. This is likely also to contribute to the delay in resolution observed after hydroxylase inhibition. This effect was shown to be Hif-dependent as dominant active Hif downregulated apoptosis. Expressing dominant active Hif specifically in neutrophils was able to decrease neutrophil apoptosis showing this effect is mediated by the neutrophils themselves. Upregulated hypoxia has been previously demonstrated to decrease neutrophil apoptosis in mammalian

systems,^{14-16,19} however this is the first time this effect has been observed *in vivo* in a whole organism. Dominant negative Hif expression did not detectably increase apoptosis levels compared to controls. This is likely to indicate that levels of Hif are low during the normal process of inflammation resolution, therefore further inhibition of this pathway does not significantly affect neutrophil apoptosis.

It is difficult to assess the relative contribution of apoptosis versus reverse migration to the clearance of neutrophils after Hif activation, because the number of apoptotic cells identified depends on unknown variables, such as the duration for which an apoptotic neutrophil can be detected before it is degraded following macrophage ingestion. However, these data suggest both are likely to play an important role in the clearance of neutrophils.

Given the potential for non-specific effects of competitive hydroxylase inhibition by DMOG, and the lack of selective inhibitors of individual PHD enzymes there were multiple possible modes of action of DMOG *in vivo*. DMOG has targets other than the HIF hydroxylases and PHD enzymes themselves have HIF independent effects, including on the NF κ B pathway.⁴⁵ By manipulating gene expression we have been able to establish a direct link between the effects of hydroxylase inhibition and Hif-1 α . Previous reports have shown that an *arnt-1* translation blocking morpholino is able to block Hif-1 α signaling.³¹ We found that morpholino mediated knock-down of Arnt-1, an obligate binding partner of Hif-1 α , is able to block the delay in inflammation resolution caused by DMOG. In addition, we found that the pro-inflammatory effects of DMOG were replicated by dominant active *hif-1ab*, and blocked by dominant negative *hif-1ab*. Dominant active *hif-1ab* delayed the resolution of inflammation to a similar degree to that of DMOG treatment alone. Interestingly, dominant active *hif-1ab* also increased the whole body neutrophil number. This might be a feature of suppression of neutrophil apoptosis during hematopoiesis, or an increase in myeloid cell production following hypoxic stimulation. This effect is not seen with either DMOG or hypoxia itself (Figure S1B and data not shown), but prolonged exposure of developing larvae to DMOG or to direct hypoxia is toxic to embryos (data not shown). This agrees with the findings in *vhl* mutants, in which increased Hif signalling leads to increased leukocyte number.⁴³ By developing a stable *UAS:da-hif-1ab* transgenic line we were able to drive the expression of *da-hif-1ab* specifically in *lyz* expressing leukocytes. We were able to demonstrate that over-activation of the Hif-1 α pathway in neutrophils alone was able to induce the delay in the resolution of neutrophilic inflammation observed when Hif-1 α was upregulated across all tissues of the embryo.

The two zebrafish homologues of human HIF-1 α had different effects on neutrophilic inflammation. Hif-1 α b was able to modulate the resolution of neutrophilic inflammation: dominant active Hif-1 α b was able to replicate the effect of hydroxylase inhibition while conversely dominant negative Hif-1 α b almost completely blocked the DMOG effect. This is consistent with Hif-1 α b being the hypoxia transcription factor responsible for the timely resolution of neutrophilic inflammation. Hif-1 α a, by contrast, had no significant effect on neutrophil behaviour in the assays we performed. Interestingly Hif-1 α a has less sequence homology to human of HIF-1 α than Hif-1 α b.⁴⁶ In particular, Hif-1 α a lacks the first conserved proline site for Phd hydroxylation, although it does have the second conserved proline site, and the Fih asparagine. The loss of complete Phd hydroxylation in Hif-1 α a may indicate a divergence of the role of Hif-1 α a in evolution away from a role in transducing the hypoxic signal in inflammatory cells.

To assess the role of hydroxylation at different sites in Hif-1 α , we assayed inflammation resolution in zebrafish larvae injected with a range of dominant Hif-1 α b constructs, in which Phd and Fih hydroxylation sites were mutated alone and in combination. Mutation of either Phd hydroxylation site reproduced the delay of inflammation resolution phenotype, consistent with a stabilization of Hif, suggesting that either site may function independently, in keeping with the recent *in vitro* crystal structure of hydroxyproline recognition by pVHL.⁴⁷ These data are consistent with Phd hydroxylation of Hif-1 α b being required for the timely resolution of neutrophilic inflammation. Whilst *in vitro* FIH/HIF interaction has been proposed to partially determine oxygen sensitivity, mutation of the Fih hydroxylation site, either alone or in combination with mutation of the Phd sites, had no detectable effect on inflammation resolution. This suggests that in zebrafish neutrophils, Phd enzymes are the critical regulators of Hif activity.

Our data show that Hif-1 α delays the resolution of inflammation in a whole organism *in vivo* model. We show for the first time that this delay in resolution is caused by suppression of the movement of neutrophils away from the site of inflammation in favour of patrolling the inflamed area, and by a decrease in neutrophil apoptosis. Furthermore, we find that hydroxylation of Hif-1 α b by Phd enzymes is required for the timely resolution of neutrophilic inflammation. By developing the stable *UAS:da-hif-1ab* transgenic line we are able to show that this depends on Hif signaling within the neutrophil. These data have important implications in understanding the role of HIF/hydroxylase signaling in innate immune responses and in addition provides an illustration of how zebrafish models might elucidate key regulators of inflammatory signaling pathways with relevance to human health.

Acknowledgements.

The authors would like to thank Catherine Loynes for assistance in establishing the techniques used in this manuscript. This work was funded by a project grant from the Wellcome Trust (Reference number: WT082909MA), an MRC Senior Clinical Fellowship to SAR (reference number: G0701932) and by A*STAR (Singapore). SRW holds a Wellcome Intermediate Fellowship (reference number: WT078244AIA). Microscopy studies were supported by a Wellcome Trust grant to the MBB/BMS Light Microscopy Facility (GR077544AIA), and the work was supported by an MRC Centre grant (G0700091).

Authorship

FJvE, SRW, MKW and SAR conceived the study and designed the experiments with PME; PWI and XW generated new transgenic reagents; PME, FJvE, PWI, MKW, SRW and SAR wrote the manuscript; CCRA assisted and advised on image processing; PME and GD performed the experiments. The authors declare no conflict of interest.

References

1. Barton GM. A calculated response: control of inflammation by the innate immune system. *J Clin Invest*. 2008;118(2):413-420.
2. Haslett C. Resolution of acute inflammation and the role of apoptosis in the tissue fate of granulocytes. *Clin Sci (Lond)*. 1992;83(6):639-648.
3. Savill JS, Wyllie AH, Henson JE, Walport MJ, Henson PM, Haslett C. Macrophage phagocytosis of aging neutrophils in inflammation. Programmed cell death in the neutrophil leads to its recognition by macrophages. *J Clin Invest*. 1989;83(3):865-875.
4. Cox G, Crossley J, Xing Z. Macrophage engulfment of apoptotic neutrophils contributes to the resolution of acute pulmonary inflammation in vivo. *Am J Respir Cell Mol Biol*. 1995;12(2):232-237.
5. Grigg JM, Savill JS, Sarraf C, Haslett C, Silverman M. Neutrophil apoptosis and clearance from neonatal lungs. *Lancet*. 1991;338(8769):720-722.
6. Uller L, Persson CG, Erjefalt JS. Resolution of airway disease: removal of inflammatory cells through apoptosis, egression or both? *Trends Pharmacol Sci*. 2006;27(9):461-466.
7. Buckley CD, Ross EA, McGettrick HM, et al. Identification of a phenotypically and functionally distinct population of long-lived neutrophils in a model of reverse endothelial migration. *J Leukoc Biol*. 2006;79(2):303-311.
8. Mathias JR, Perrin BJ, Liu TX, Kanki J, Look AT, Huttenlocher A. Resolution of inflammation by retrograde chemotaxis of neutrophils in transgenic zebrafish. *J Leukoc Biol*. 2006;80(6):1281-1288.
9. Brown SB, Tucker CS, Ford C, Lee Y, Dunbar DR, Mullins JJ. Class III antiarrhythmic methanesulfonanilides inhibit leukocyte recruitment in zebrafish. *J Leukoc Biol*. 2007;82(1):79-84.
10. Hall C, Flores MV, Storm T, Crosier K, Crosier P. The zebrafish lysozyme C promoter drives myeloid-specific expression in transgenic fish. *BMC Dev Biol*. 2007;7:42.
11. Lee A, Whyte MK, Haslett C. Inhibition of apoptosis and prolongation of neutrophil functional longevity by inflammatory mediators. *J Leukoc Biol*. 1993;54(4):283-288.
12. Colotta F, Re F, Polentarutti N, Sozzani S, Mantovani A. Modulation of granulocyte survival and programmed cell death by cytokines and bacterial products. *Blood*. 1992;80(8):2012-2020.
13. Sabroe I, Dower SK, Whyte MK. The role of Toll-like receptors in the regulation of neutrophil migration, activation, and apoptosis. *Clin Infect Dis*. 2005;41 Suppl 7:S421-426.
14. Hannah S, Mecklenburgh K, Rahman I, et al. Hypoxia prolongs neutrophil survival in vitro. *FEBS Lett*. 1995;372(2-3):233-237.
15. Mecklenburgh KI, Walmsley SR, Cowburn AS, et al. Involvement of a ferroprotein sensor in hypoxia-mediated inhibition of neutrophil apoptosis. *Blood*. 2002;100(8):3008-3016.
16. Walmsley SR, Print C, Farahi N, et al. Hypoxia-induced neutrophil survival is mediated by HIF-1alpha-dependent NF-kappaB activity. *J Exp Med*. 2005;201(1):105-115.
17. Cramer T, Yamanishi Y, Clausen BE, et al. HIF-1alpha is essential for myeloid cell-mediated inflammation. *Cell*. 2003;112(5):645-657.
18. Peyssonnaud C, Datta V, Cramer T, et al. HIF-1alpha expression regulates the bactericidal capacity of phagocytes. *J Clin Invest*. 2005;115(7):1806-1815.

19. Walmsley SR, Cowburn AS, Clatworthy MR, et al. Neutrophils from patients with heterozygous germline mutations in the von Hippel Lindau protein (pVHL) display delayed apoptosis and enhanced bacterial phagocytosis. *Blood*. 2006;108(9):3176-3178.
20. Epstein AC, Gleadle JM, McNeill LA, et al. *C. elegans* EGL-9 and mammalian homologs define a family of dioxygenases that regulate HIF by prolyl hydroxylation. *Cell*. 2001;107(1):43-54.
21. Bruick RK, McKnight SL. A conserved family of prolyl-4-hydroxylases that modify HIF. *Science*. 2001;294(5545):1337-1340.
22. Kaelin WG, Jr., Ratcliffe PJ. Oxygen sensing by metazoans: the central role of the HIF hydroxylase pathway. *Mol Cell*. 2008;30(4):393-402.
23. Semenza GL, Wang GL. A nuclear factor induced by hypoxia via de novo protein synthesis binds to the human erythropoietin gene enhancer at a site required for transcriptional activation. *Mol Cell Biol*. 1992;12(12):5447-5454.
24. Wenger RH. Cellular adaptation to hypoxia: O₂-sensing protein hydroxylases, hypoxia-inducible transcription factors, and O₂-regulated gene expression. *FASEB J*. 2002;16(10):1151-1162.
25. Jaakkola P, Mole DR, Tian YM, et al. Targeting of HIF- α to the von Hippel-Lindau ubiquitylation complex by O₂-regulated prolyl hydroxylation. *Science*. 2001;292(5516):468-472.
26. Renshaw SA, Loynes CA, Trushell DM, Elworthy S, Ingham PW, Whyte MK. A transgenic zebrafish model of neutrophilic inflammation. *Blood*. 2006;108(13):3976-3978.
27. Nusslein-Volhard C DR. Zebrafish: A Practical Approach (ed 1st ed). Oxford: Oxford University Press; 2002.
28. Loynes CA, Martin JS, Robertson A, et al. Pivotal Advance: Pharmacological manipulation of inflammation resolution during spontaneously resolving tissue neutrophilia in the zebrafish. *J Leukoc Biol*. 2010;87(2):203-212.
29. Sidi S, Sanda T, Kennedy RD, et al. Chk1 suppresses a caspase-2 apoptotic response to DNA damage that bypasses p53, Bcl-2, and caspase-3. *Cell*. 2008;133(5):864-877.
30. Kwan KM, Fujimoto E, Grabher C, et al. The Tol2kit: a multisite gateway-based construction kit for Tol2 transposon transgenesis constructs. *Dev Dyn*. 2007;236(11):3088-3099.
31. Prash AL, Tanguay RL, Mehta V, Heideman W, Peterson RE. Identification of zebrafish ARNT1 homologs: 2,3,7,8-tetrachlorodibenzo-p-dioxin toxicity in the developing zebrafish requires ARNT1. *Mol Pharmacol*. 2006;69(3):776-787.
32. Manotham K, Tanaka T, Ohse T, et al. A biologic role of HIF-1 in the renal medulla. *Kidney Int*. 2005;67(4):1428-1439.
33. Epstein A, Gleadle J, McNeill L, et al. *C. elegans* EGL-9 and mammalian homologs define a family of dioxygenases that regulate HIF by prolyl hydroxylation. *Cell*. 2001;107(1):43-54.
34. Chan DA, Sutphin PD, Yen SE, Giaccia AJ. Coordinate regulation of the oxygen-dependent degradation domains of hypoxia-inducible factor 1 α . *Mol Cell Biol*. 2005;25(15):6415-6426.
35. Linke S, Stojkoski C, Kewley RJ, Booker GW, Whitelaw ML, Peet DJ. Substrate requirements of the oxygen-sensing asparaginyl hydroxylase factor-inhibiting hypoxia-inducible factor. *J Biol Chem*. 2004;279(14):14391-14397.
36. Krauss S, Concordet JP, Ingham PW. A functionally conserved homolog of the *Drosophila* segment polarity gene hh is expressed in tissues with polarizing activity in zebrafish embryos. *Cell*. 1993;75(7):1431-1444.

37. Thisse C, Thisse B. High-resolution in situ hybridization to whole-mount zebrafish embryos. *Nat Protoc.* 2008;3(1):59-69.
38. Gray CA, Loynes CA, Whyte MK, Crossman DC, Renshaw SA, Chico TJ. Simultaneous intravital imaging of macrophage and neutrophil behaviour during inflammation using a novel transgenic zebrafish. *Thrombosis and Haemostasis.* 2010;In press.
39. Le Guyader D, Redd MJ, Colucci-Guyon E, et al. Origins and unconventional behavior of neutrophils in developing zebrafish. *Blood.* 2008;111(1):132-141.
40. Howie SE, Harrison DJ, Wyllie AH. Lymphocyte apoptosis--mechanisms and implications in disease. *Immunol Rev.* 1994;142:141-156.
41. Ando R, Hama H, Yamamoto-Hino M, Mizuno H, Miyawaki A. An optical marker based on the UV-induced green-to-red photoconversion of a fluorescent protein. *Proc Natl Acad Sci U S A.* 2002;99(20):12651-12656.
42. Lieschke GJ, Oates AC, Crowhurst MO, Ward AC, Layton JE. Morphologic and functional characterization of granulocytes and macrophages in embryonic and adult zebrafish. *Blood.* 2001;98(10):3087-3096.
43. van Rooijen E, Voest EE, Logister I, et al. Zebrafish mutants in the von Hippel-Lindau tumor suppressor display a hypoxic response and recapitulate key aspects of Chuvash polycythemia. *Blood.* 2009;113(25):6449-6460.
44. Weisel KC, Bautz F, Seitz G, Yildirim S, Kanz L, Mohle R. Modulation of CXC chemokine receptor expression and function in human neutrophils during aging in vitro suggests a role in their clearance from circulation. *Mediators of inflammation.* 2009;2009:790174.
45. Cummins EP, Berra E, Comerford KM, et al. Prolyl hydroxylase-1 negatively regulates IkappaB kinase-beta, giving insight into hypoxia-induced NFkappaB activity. *Proc Natl Acad Sci U S A.* 2006;103(48):18154-18159.
46. Rojas DA, Perez-Munizaga DA, Centanin L, et al. Cloning of hif-1alpha and hif-2alpha and mRNA expression pattern during development in zebrafish. *Gene Expr Patterns.* 2007;7(3):339-345.
47. Hon WC, Wilson MI, Harlos K, et al. Structural basis for the recognition of hydroxyproline in HIF-1 alpha by pVHL. *Nature.* 2002;417(6892):975-978.

Figure legends

Figure 1: DMOG delays resolution of neutrophilic inflammation. (A-B) Fluorescent neutrophil numbers in the *mpx:GFP* line were counted at 6, 24 and 48 hpi in anesthetized embryos. 6hpi is the timepoint of maximal neutrophil recruitment. By 24hpi neutrophilic inflammation has resolved in wildtype embryos. At 4hpi, fish were treated with 100µM DMOG (B) or with DMSO as vehicle control (A). Data shown are individual embryos for each line, n = 18 performed as 3 independent experiments. (C) Fluorescence photomicrographs of 8 zebrafish tails from (upper panel) control (DMSO) and (lower panel) DMOG treated larvae. Imaged at 24hpi, 2X magnification on a Nikon TE2000U inverted microscope at constant exposure. (D,E) Overlaid fluorescence and brightfield photomicrographs of injured 3dpf embryos at 6hpi and 24hpi (D) or uninjured 3dpf and 4dpf embryos (E) after treatment at 3dpf with DMSO and DMOG. Imaged at 2X magnification on a Nikon TE2000U inverted microscope at constant exposure. (F) 6hpi timepoint neutrophil counts, in DMSO and DMOG treated zebrafish embryos. Data shown are mean ± SEM, n = 18 performed as 3 independent experiments. (G) The resolution of the cellular component of inflammation is decreased in DMOG treated embryos, expressed as percentage change in neutrophil number between 6 and 24hpi. Data shown are mean ± SEM, n = 18 performed as 3 independent experiments. P values were calculated using one-way ANOVA and Bonferroni multiple

comparison test, * $p < 0.05$, ** $p < 0.01$, and *** $p < 0.001$. (H) A photomicrograph of a typical tracking experiment with arrows indicating the path of neutrophil movement over a 1 hour timelapse during the recruitment phase of inflammation (1-2hpi). No difference was observed in the speed of neutrophil migration (I) or meandering index (displacement/path length) (J) in DMOG treated larvae compared to DMSO controls. Data shown are mean \pm SEM, $n = 18$ performed as 3 independent experiments. (K) TUNEL and TSA co-localisation shows the percentage of neutrophils at the injury site undergoing apoptosis. Data shown are mean \pm SEM, $n = 3$ performed as independent experiments each containing 35-40 embryos per treatment group.

Figure 2: DMOG retains neutrophils in the region of tissue injury. (A) Photomicrographs of a 3dpf photoconverted, DMSO treated, *lyz:Kaede* embryo at 0 hours post conversion (hpc). The white dashed line indicates the border of the site of transection area. The cells to the right of the line were photoconverted, leaving them with red fluorescence rather than green. The lower fluorescent panel shows the area of interest where neutrophils migrated away from the injury site shown in subsequent figure (D). (B) Photomicrographs of the same embryo as in (A) at 0hpc and 3.5hpc. The red channel only is shown, as a binary image. Between 0 and 3.5hpc photoconverted cells have migrated away from the site of transection. (C) Photomicrographs of a DMOG treated embryo at 0 and 3.5hpc converted into black and white. Fewer photoconverted leukocytes have migrated away from the site of transection. (D) A plot showing the number of photoconverted leukocytes leaving the area of transection over 3.5hpc in DMSO and DMOG treated embryos. Data shown are mean \pm SEM, $n = 9$ performed as 2 independent experiments. Line of best fit shown is calculated by linear regression. P value shown is for the difference between the 2 slopes.

Figure 3: DMOG treatment causes a change in direction of neutrophil movement independent of neutrophil speed and meandering. (A) Photomicrographs of a 3dpf photoconverted, DMSO treated, *lyz:Kaede* embryo at 0 hours post conversion (hpc). The white box indicates the area of photoconverted, neutrophils. The lower panel shows the regions to which neutrophils migrated in subsequent figures (D-F). (B) Photomicrographs of examples of DMSO (upper panel) and DMOG (lower panel) embryos with the tracks of neutrophils over the first 3.5hpc shown. The dashed line indicates the outline of the embryo. (C) Tracking of neutrophils over the first 3.5hpc in the resolution phase of inflammation showed no difference in the speed of neutrophil migration (upper panel) or meandering index (displacement/path length) (lower panel) in DMOG treated larvae compared to DMSO controls. (D) Leukocytes leave the photoconversion site at the same rate in DMSO and DMOG treated embryos over 3.5hpc. (E) The number of photoconverted leukocytes moving away from the wound is shown over 3.5hpc in DMSO and DMOG treated embryos. (F) More neutrophils remain and patrol the injury site in DMOG treated embryos, since a greater number of leukocytes move within the injury region, ventrally away from the patch area. (D-F) Data shown are mean \pm SEM, $n = 14$ performed as 3 independent experiments. Line of best fit shown is calculated by linear regression. P values shown are the differences between the 2 slopes.

Figure 4: DMOG induced delay in inflammation resolution is blocked by genetic inhibition of the Hif-1 α pathway. (A) The 24hpi neutrophil counts in the *mpx:GFP* line at 2dpf following injection with control and *arnt-1* morpholinos. DMSO and DMOG treatment was performed at 4hpi. Data shown are mean \pm SEM, $n = 12$ performed as 2 independent experiments. (B-E) 177pg of dominant negative *hif-1 α* RNA was injected into the 1 cell stage zebrafish *mpx:GFP* embryos and neutrophil counts were performed at 24hpi after tail transection at 2dpf. (B) Injection of dominant negative *hif-1 α* abrogated the increase in neutrophil number at the site of injury at 24hpi seen with DMOG treatment, whilst embryos injected with phenol red as a negative control, or dominant negative *hif-1 α* alone exhibited a significant increase in neutrophil number after DMOG treatment. Data shown are mean \pm SEM, $n = 24$ performed as 2 independent experiments. P values were calculated using one-way ANOVA and Bonferroni multiple comparison test, where * represented $p < 0.05$, ** $p < 0.01$, and ***, $p < 0.001$. (C) Injection of dominant negative *hif-1 α* variants led to no significant difference in total neutrophil number at 2dpf compared to

phenol red injected negative control embryos. Data shown are mean \pm SEM, n = 36 performed as 3 independent experiments. (D) Injection of dominant negative *hif-1 α* caused no significant change in percentage of neutrophils at the injury site co-labeling with TUNEL stain (12hpi injured at 2dpf). Data shown are mean \pm SEM, n = 4 performed as independent experiments containing 5-25 embryos per injection group per repeat. (E-F) Dominant negative *hif-1 α* can block the increased neutrophil retention at the site of injury caused by DMOG treatment. Embryos were injected with dominant negative *hif-1 α* , grown to 3dpf and imaged 3.5 hours after photoconversion, with only the red channel shown, as a binary image. (E, left panels) in DMSO treated larvae red-labeled neutrophils have migrated away from the site of transection. (E, right panel) in DMOG treated larvae, red-labeled neutrophils also move away from the site of transection. (F) The number of red (photoconverted) lysC labeled cells leaving the area of transection at 6hpi over a time period of 3.5hpc in DMSO and DMOG treated embryos at 2dpf that were injected at the 1 cell stage with dominant negative *hif-1 α* . Data shown are mean \pm SEM, n = 14 performed as 3 independent experiments. Line of best fit shown is calculated by linear regression. P value shown is the difference between the 2 slopes.

Figure 5: Dominant active *hif-1 α* delays resolution of neutrophilic inflammation. (A) Partial protein alignment showing the conserved hydroxylation sites of Hif-1 α . Dominant active *hif-1 α* has the following non-hydroxylatable mutations: Hif-1 α b P402A, P564G, N804A and Hif-1 α a P493G, N678A (Hif-1 α a lacks the first proline hydroxylation residue). (B-F) Dominant active forms of *hif-1 α* RNA (177pg) were injected into the 1 cell stage zebrafish *mpx:GFP* embryos, tailfin transection performed at 2dpf, and neutrophils counted at 24hpi. (B) Dominant active *hif-1 α* caused a significant increase in neutrophil number in the absence of DMOG treatment compared to phenol red injected negative controls. Dominant active *hif-1 α* b alone was able to recapitulate the DMOG phenotype, whilst dominant active *hif-1 α* a homologue did not. Data shown are mean \pm SEM, n = 24 performed as 2 independent experiments. P values were calculated using one-way ANOVA and Bonferroni multiple comparison test, where * represented p<0.05, ** p<0.01, and ***, p<0.001. (C) Injection of dominant active *hif-1 α* variants led to a significant increase in total neutrophil numbers at 2dpf. Data shown are mean \pm SEM, n = 36 performed as 3 independent experiments. (D) Injection of dominant active *hif-1 α* variants did not alter the recruitment of neutrophils to the injury site after 6hpi when the tail was transected at 2dpf. Data shown are mean \pm SEM, n = 24 performed as 2 independent experiments. P values were calculated using one-way ANOVA and Bonferroni multiple comparison test. (E) Injection of dominant active *hif-1 α* led to a significant decrease in percentage of neutrophils at the injury site co-labeled with TUNEL apoptosis staining 12hpi when injured at 2dpf. Data shown are mean \pm SEM, n = 4 performed as independent experiments containing 10-25 embryos per injection group per repeat. (F) The number of red (photoconverted) lysC labeled cells leaving the area of transection at 6hpi over a time period of 3.5hpc in phenol red and dominant active *hif-1 α* injected embryos at 2dpf. Data shown are mean \pm SEM, n = 14 performed as 3 independent experiments. Line of best fit shown is calculated by linear regression. P value shown is the difference between the 2 slopes. (G) Injection of *hif-1 α* b with each hydroxylation site mutated individually shows that the asparagine hydroxylation site of Fih is not required for resolution of neutrophilic inflammation. Mutation of either proline hydroxylation site of Hif-1 α b was sufficient to lead to the decrease in neutrophil inflammation resolution. Data shown are mean \pm SEM, n = 24 performed as 2 independent experiments. (H) *Tg(lyz:Gal4)i252;Tg(UAS:da-hif-1 α b-IRES-GFP)i218* positive embryos and wildtype siblings underwent tailfin transection at 3dpf. Data shown are 24hpi TSA positive neutrophil counts, mean \pm SEM, n = 30 performed as 3 independent experiments. (I) *Tg(lyz:Gal4)i252;Tg(UAS:da-hif-1 α b-IRES-GFP)i218* positive embryos had a lower rate of neutrophil apoptosis analyzed by TUNEL staining at 12hpi after tail transection at 3dpf. Data shown are mean \pm SEM, n = 3 performed as independent experiments containing 9-40 embryos per treatment group per repeat.

Figure 1

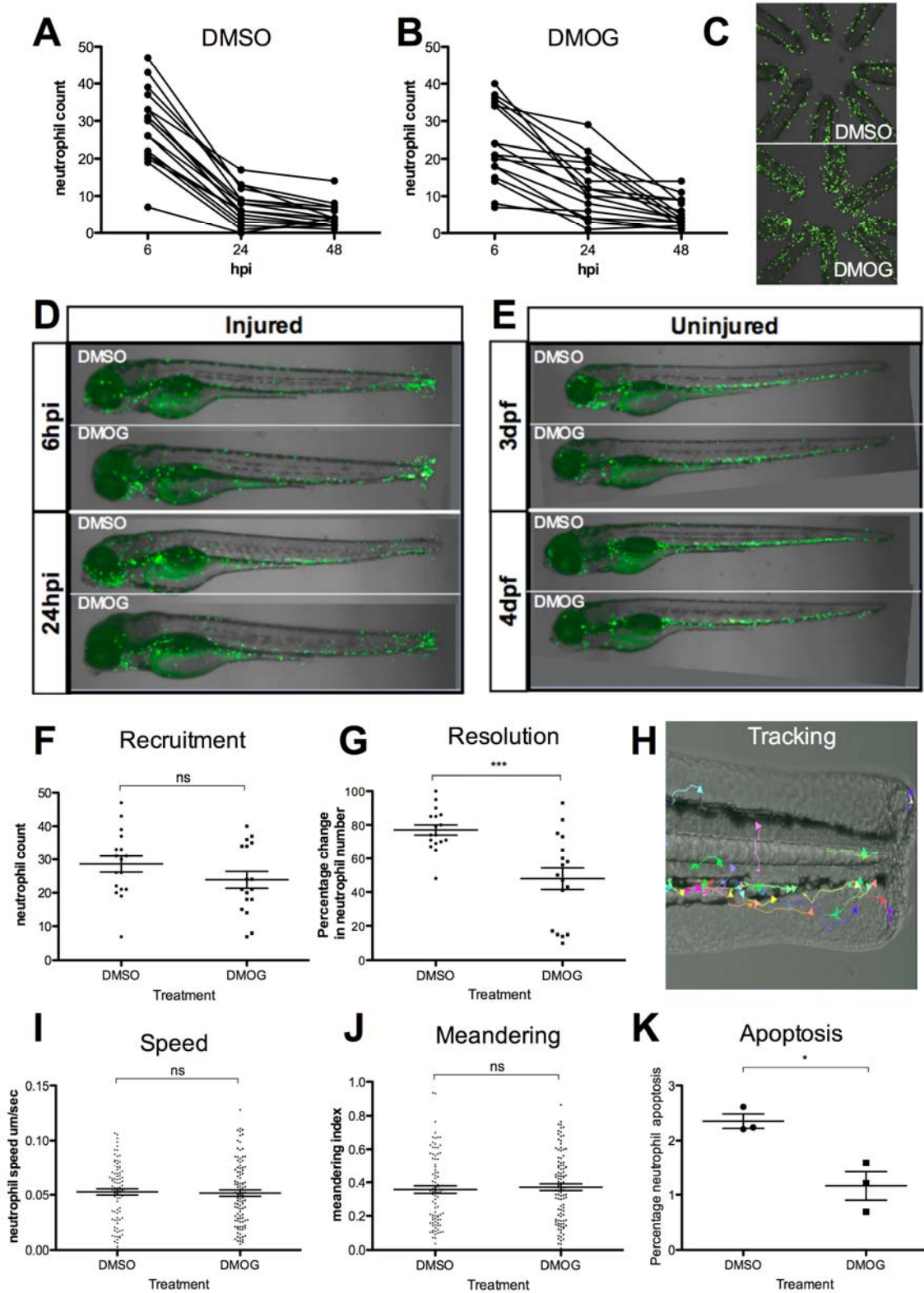


Figure 2

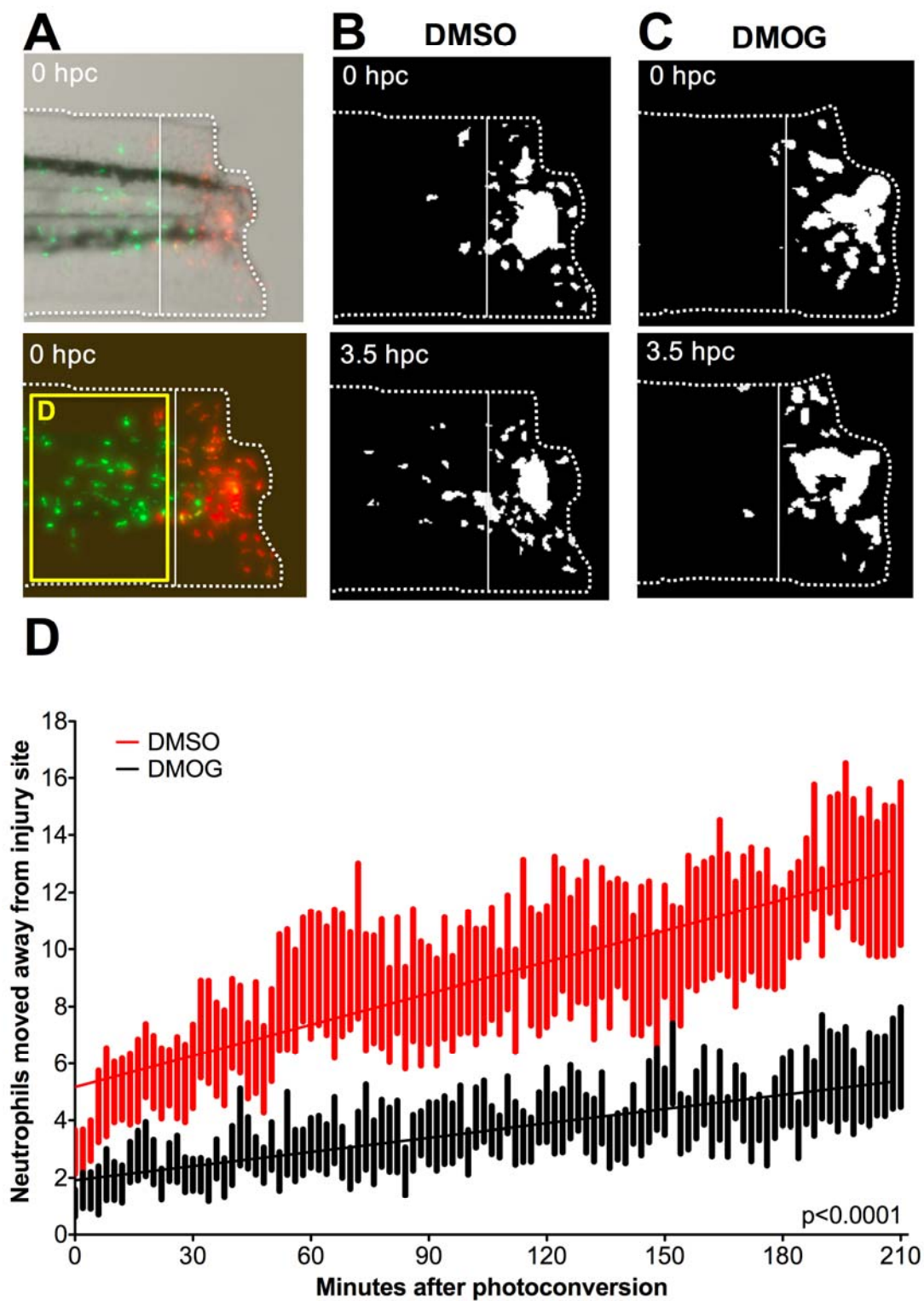


Figure 3

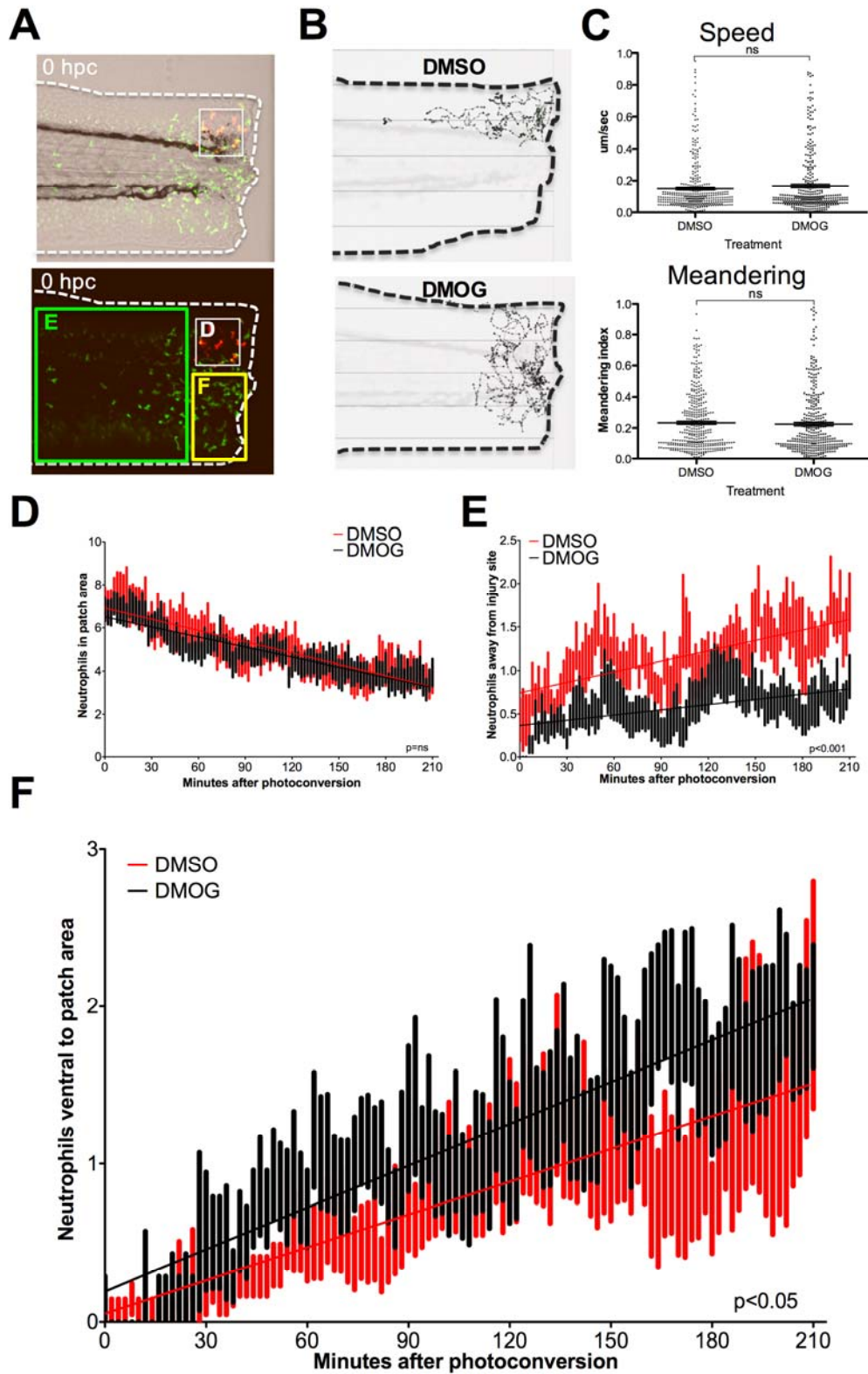


Figure 4

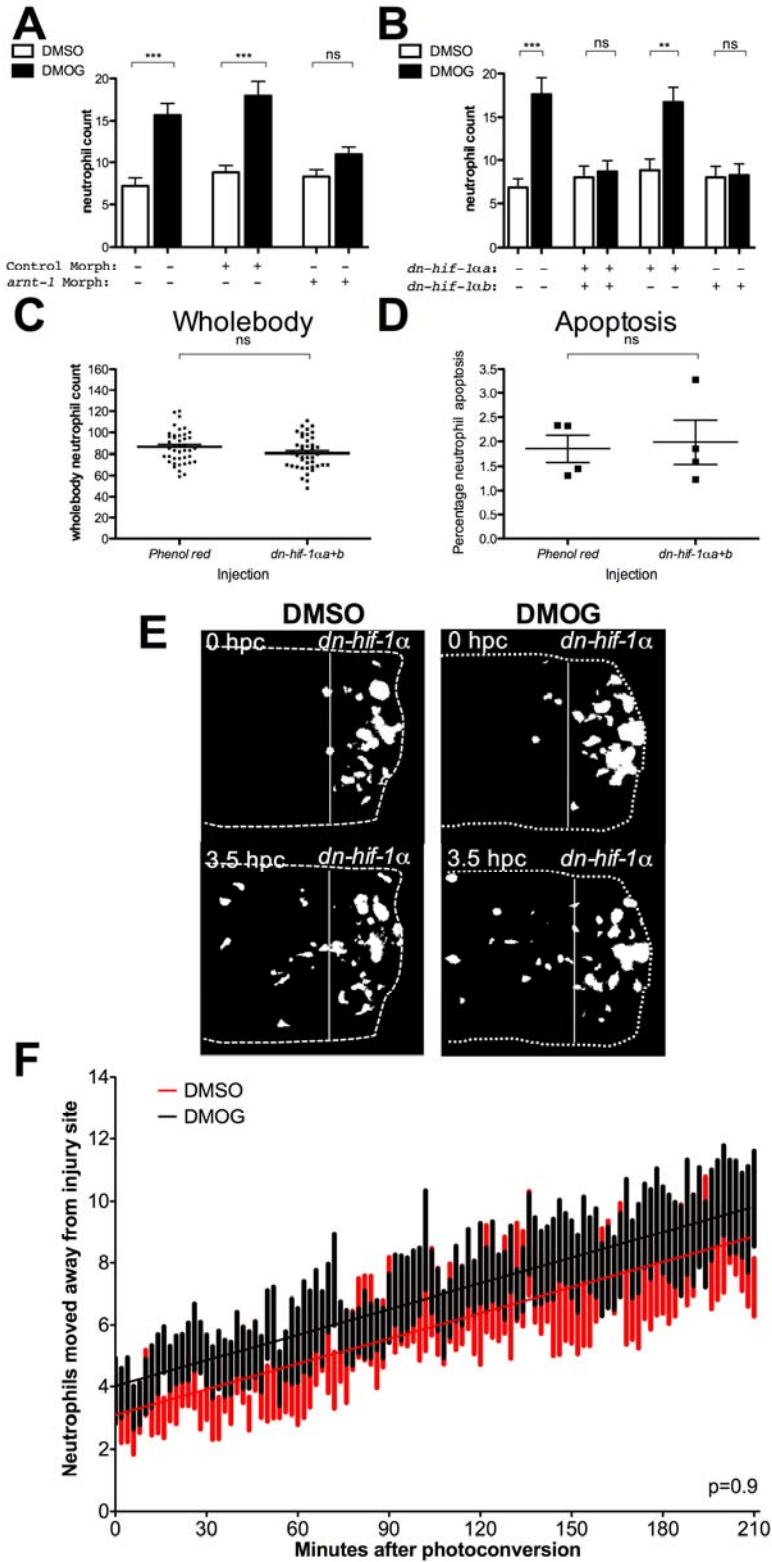
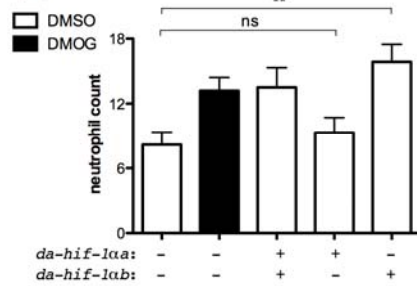


Figure 5

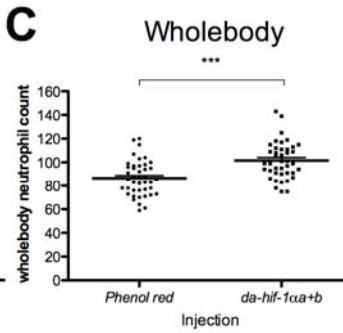
A

	:**:::~::~*~	*****~::~*	.*****.~
Zebrafish HIF-1 α A	ALTV-----AD	LDLEMLAPYIPM	HDCEVNAPVIG
Zebrafish HIF-1 α B	ALTVLAPAAAGD	LDLEMLAPYIPM	YDCEVNAPVQD
Fugu HIF-1 α	ALTLAPAAAGD	LDLEMLAPYISM	DDCEVNAPLQG
Human HIF-1 α	ALTLAPAAAGD	LDLEMLAPYIPM	YDCEVNAPIQG
Mouse HIF-1 α	ALTLAPAAAGD	LDLEMLAPYIPM	YDCEVNAPIQG
Rat HIF-1 α	ALTLAPAAAGD	LDLEMLAPYIPM	YDCEVNAPIQG
Chick HIF-1 α	ALTVLAPAAAGD	LDLEMLAPYIPM	YDCEVNAPIQG
Frog HIF-1 α	SLTVLAPDAGD	LDLEMLAPYIPM	YDCEVNAPVHG

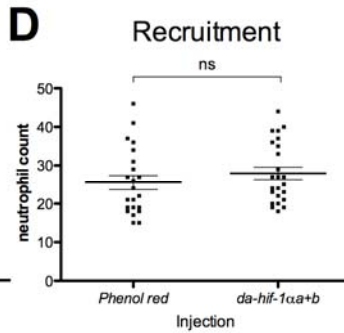
B



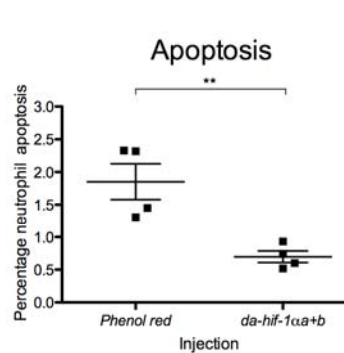
C



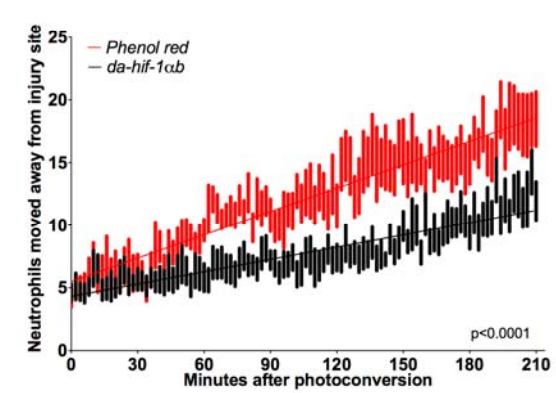
D



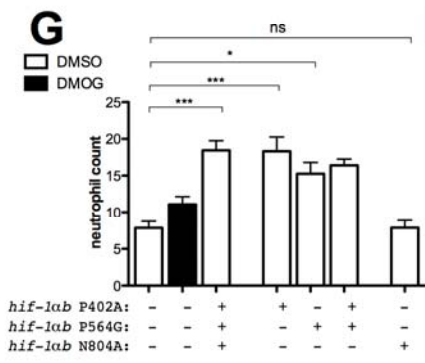
E



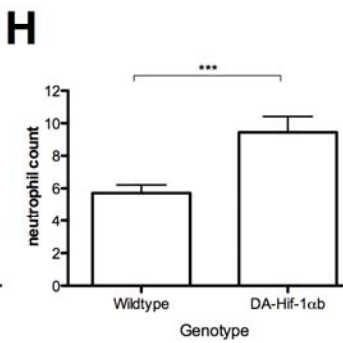
F



G



H



I

